Research Square

Preprints are preliminary reports that have not undergone peer review.
They should not be considered conclusive, used to inform clinical practice,
or referenced by the media as validated information.

Spatio-Temporal Dynamics of Land Surface Temperature in the Theri Soil Landscape and Its Thermal Association with Surrounding Land Uses

A. Anto Rashwin

antorashwin@gmail.com

Tamil Nadu Agricultural University

J. Ramachandran

Tamil Nadu Agricultural University

Research Article

Keywords: Land surface temperature, Theri soil, Landsat 8, Thermal landscape, Land use/land cover, Spatial thermal association

Posted Date: November 11th, 2026

DOI: https://doi.org/10.21203/rs.3.rs-11330460/v1

License: This work is licensed under a Creative Commons Attribution 4.0 International License.
Read Full License

Additional Declarations: No competing interests reported.

Spatio-Temporal Dynamics of Land Surface Temperature in the Theri Soil Landscape and Its Thermal Association with Surrounding Land Uses

A. Anto Rashwin[1*] and J. Ramachandran[2*]

[1]Department of Environmental Sciences, Tamil Nadu Agricultural University, Coimbatore 641 003, Tamil Nadu, India

[2]Department of Soil and Water Conservation Engineering, Tamil Nadu Agricultural University, Coimbatore 641 003, Tamil Nadu, India

*Corresponding authors' email addresses:

AAR: antorashwin@gmail.com

JR: ramachandran.j@tnau.ac.in

Abstract

Land surface temperature (LST) provides an important indicator of surface thermal behaviour and reveals differences in energy exchange across heterogeneous landscapes. This study investigated the spatio-temporal dynamics of LST over the Theri soil landscape of southern Tamil Nadu, India, and its thermal association with surrounding built-up, vegetation, agricultural and barren land uses across multiple spatial scales. Landsat 8 imagery from 2015–2024 was processed in Google Earth Engine to derive LST and assess thermal relationships within 0–1, 1–2 and 2–5 km zones from the Theri soil boundary. Temporal analysis, correlation matrices and pairwise scatter plots were used to evaluate thermal synchrony and spatial dependence, complemented by ground observations from representative landscape conditions. Theri soil exhibited substantial seasonal and interannual variability and generally higher LST than vegetated and agricultural surfaces. The strongest association occurred between Theri soil and built-up land at 1 km ($r = 0.92$), decreasing to 0.85 and 0.82 at 2 and 5 km, respectively. Vegetation and agriculture also remained strongly associated with Theri soil, whereas barren land exhibited a strong but non-monotonic relationship across spatial scales. Field observations revealed pronounced thermal contrasts, with exposed red sand reaching 57.3 °C compared with substantially lower temperatures under vegetated conditions. The findings demonstrate that Theri soil forms a distinct yet thermally interconnected landscape unit and highlight the importance of spatial context, vegetation cover and surrounding land-use characteristics in understanding its thermal behaviour.

Keywords: Land surface temperature; Theri soil; Landsat 8; Thermal landscape; Land use/land cover; Spatial thermal association

1 Introduction

Land Surface Temperature (LST) is a fundamental biophysical variable that represents the thermal state of the Earth's land surface and provides an integrated response to the exchanges of radiation, heat and moisture between the land surface and the lower atmosphere (Z. Li et al., 2023). Unlike conventional air-temperature observations, which are generally obtained from a limited number of meteorological stations, remotely sensed LST provides spatially continuous information on the thermal characteristics of heterogeneous landscapes. Land surface temperature (LST) is a key indicator of the thermal state of the land surface and reflects the exchange and partitioning of energy between the land and atmosphere (Taheri et al., 2022). Satellite-derived LST provides spatially distributed observations that enable thermal variability to be examined across heterogeneous landscapes and through time (Firozjaei et al., 2022). It has consequently been applied extensively in studies of land–atmosphere interactions, surface energy balance, hydrological processes, vegetation dynamics, drought, agricultural water management, urban climate and environmental change (Z.-L. Li et al., 2013). Remotely sensed LST has also been used as an indicator of surface soil-moisture conditions and drought stress, providing an indirect means of assessing hydrothermal variability over areas where conventional observations are spatially limited (Cammalleri & Vogt, 2015). Advances in thermal remote sensing have further improved the capacity to characterize surface thermal conditions at local and regional scales, while Landsat provides a useful spatial resolution for investigating thermal contrasts within heterogeneous landscapes. The availability of cloud-based processing environments has additionally made multi-temporal Landsat LST analysis more practical and reproducible (Ermida et al., 2020).

LST is not determined by land-cover class alone but by the combined effects of atmospheric forcing and surface characteristics, including emissivity, albedo, roughness, soil texture, mineral composition, vegetation fraction and moisture availability. Among these controls, soil moisture has a particularly important role because it influences both the physical properties of soil and the partitioning of available energy between sensible and latent heat. A soil water–heat coupling model showed that a 1% decrease in soil moisture could increase soil surface temperature by approximately 0.08–0.43 °C, while greater moisture availability reduced temperature variability (Zhang et al., 2022). At a broader climatic scale, net radiation, soil moisture and atmospheric humidity together explained approximately 92% of long-term LST variability, demonstrating that surface thermal patterns are strongly governed by coupled water–energy processes rather than by temperature forcing alone (Jiang et al., 2023).

Vegetation provides an important counteracting control through canopy shading, increased surface roughness and evapotranspiration. Its cooling effect, however, varies with vegetation density, climatic conditions and water availability. Vegetation abundance, spatial configuration and landscape context can influence both the magnitude and spatial extent of surface cooling (Ziter et al., 2019a). A global review of LULC–LST studies similarly found that built-up surfaces commonly exhibit among the highest LST values, followed by barren surfaces, whereas vegetation and water bodies generally show lower surface temperatures (Nega & Balew, 2022). Recent evidence from tropical environments further indicates that vegetation-cover changes can modify surface temperature, with the response becoming particularly dependent on water availability in dryland environments (Feldman et al., 2023). These thermal contrasts are also evident in agricultural and human-modified landscapes. In the lower Himalayan region, mean LST reached 35.76 °C in built-up areas and 28.08 °C on bare soil, while agricultural and vegetated surfaces generally exhibited lower temperatures (Ullah et al., 2023). In Aligarh, NDVI showed a strong negative relationship with LST, whereas NDBI and bareness indices were positively associated with surface temperature, demonstrating the combined influence of vegetation density and exposed or built-up surfaces (Khan et al., 2025). In Malang, a 0.1 increase in NDBI was associated with a 1.075 °C increase in LST, whereas a 0.1 increase in NDVI corresponded to a 0.339 °C decrease (Hasyim et al., 2025). These findings demonstrate that surface temperature reflects the interaction of vegetation, exposed ground, built-up materials and moisture conditions rather than the effect of any single land-cover characteristic.

The importance of these controls becomes particularly pronounced in sandy and semi-arid environments, where sparse vegetation, rapid drainage and strong surface exposure can favour intense daytime heating. In semi-arid Indian cities, soil moisture showed a closer association with surface urban heat intensity than vegetation condition, and high LST was frequently observed in peripheral areas where dry surfaces acted as important thermal sources (Shahfahad et al., 2023). Experimental observations from gravel–sand systems likewise demonstrated a significant negative relationship between soil moisture and soil temperature, with increased moisture enhancing heat conduction and buffering extreme surface-temperature fluctuations (Han et al., 2025). Such evidence indicates that the thermal behaviour of exposed sandy surfaces must be considered in relation to moisture availability and surrounding surface conditions.

The Theri soil landscapes of southern Tamil Nadu provide a distinctive setting in which these thermal relationships can be examined. Theri terrains comprise red sandy dune formations distributed across the southern coastal and inland tracts of Tamil Nadu, with important occurrences in Thoothukudi district (Venugopal et al., 2024), including the Kuthiraimozhi region. The deposits are characterized by loose sandy materials containing

abundant quartz and feldspar together with heavy minerals such as ilmenite, rutile, garnet, magnetite and hematite. Their characteristic reddish colour has been associated with weathering, leaching and oxidation of iron-bearing minerals. Investigations of the Kuthiraimozhi deposits have documented their distinctive textural, mineralogical and geochemical characteristics and established their significance as a distinctive sedimentary landscape (Venu & Velmayil, 2021). The sandy and highly permeable nature of these formations also makes their relationship with surface moisture and groundwater processes environmentally important. Within and around the Theri formations, exposed red sand occurs alongside natural and planted vegetation, agricultural fields, barren surfaces, settlements and other human-modified land uses. This juxtaposition creates strong contrasts in surface properties over relatively short distances. Consequently, the thermal response of exposed Theri sand may differ substantially from that of vegetated or cultivated surfaces, while all surfaces may simultaneously respond to common seasonal atmospheric forcing. The thermal behaviour of Theri therefore needs to be considered as a landscape-level phenomenon, rather than simply as the temperature characteristic of an individual soil class.

Recent LST investigations provide evidence that such landscape context can be important. In New Town Kolkata, changes in LULC composition were accompanied by substantial changes in LST, demonstrating the close association between land-cover transformation and surface thermal conditions in an Indian landscape (Mahata et al., 2024). Similarly, analyses of Indian landscapes have demonstrated significant relationships among LULC, NDVI and LST, confirming that vegetation condition and land-cover composition contribute substantially to spatial thermal variability (Singh et al., 2024). At a broader scale, a systematic assessment of LULC–LST studies has shown that the magnitude of thermal differences depends on land-cover characteristics as well as landscape configuration and environmental context (Patel et al., 2024). However, most existing studies have concentrated on urban, peri-urban, agricultural or generalized semi-arid environments rather than distinctive red sandy-dune systems such as the Theri landscape. An important unresolved issue is therefore the spatial scale of thermal association. In a heterogeneous landscape, neighbouring land-use classes may exhibit similar temporal temperature fluctuations because they are exposed to common meteorological conditions, even though their absolute LST values differ because of surface-specific characteristics. Conversely, thermal associations may weaken with increasing distance as local surface controls become less influential. Buffer- and gradient-based studies provide evidence for such distance dependence. In Krakow, urban park cores were approximately 2.1–2.6 °C cooler than their 150 m buffers and approximately 2.6–3.3 °C cooler than their 300 m buffers (Głowienka & Kucza, 2026). Along an urban–rural gradient in Guangzhou–Foshan, LST decreased rapidly near the urban boundary before the rate of decrease became progressively smaller farther from the urban area (S. Zhou et al.,

2023). Similarly, analysis of greenery and water bodies in Rajshahi demonstrated that cooling magnitude varied according to feature size, surrounding land-use composition and distance from the cooling feature (Faridatul et al., 2025). These findings support the use of multiple spatial zones when evaluating the thermal association of a distinctive surface with its surroundings.

The distinction between thermal association and thermal causation is particularly important in this context. A strong correlation between Theri LST and the temperature of a neighbouring land-use class does not necessarily demonstrate that one surface directly heats or cools the other. Similar temporal patterns may instead arise from shared atmospheric forcing, seasonal moisture conditions, vegetation phenology or spatial proximity. LULC explained approximately 26–64% of LST variation in Ilorin during 2002–2020, but the strength of the relationship varied spatially and temporally, demonstrating that LST–LULC relationships are context dependent (Njoku & Tenenbaum, 2022). Likewise, multi-temporal analysis in Phnom Penh reported LST values ranging approximately from 20 to 69 °C and showed that the response of surface temperature to LULC change varied among locations rather than following a single uniform pattern (Mohiuddin & Mund, 2023). These observations indicate that thermal synchrony and spatial association should be interpreted within their environmental context rather than as evidence of a simple one-way thermal influence. Landsat 8 is particularly suitable for investigating these relationships because its OLI/TIRS configuration provides multispectral information for characterizing surface conditions together with thermal infrared observations for LST retrieval. Band 10 is commonly preferred for Landsat 8 thermal analysis because of the greater calibration uncertainty associated with Band 11 (Hasyim et al., 2025). Landsat-based spectral indices and thermal information can also be processed efficiently within Google Earth Engine, enabling multi-scene analysis and spatial extraction across defined landscape zones (Roy & Bari, 2022). Emissivity estimation remains an important consideration, particularly where exposed soil and vegetation occur together. Recent work using NDVI-based emissivity in Google Earth Engine reported improved LST precision compared with ASTER-GED-based emissivity, although accuracy varied among surface types and was lower for mixed surfaces (Bobáľová & Opravil, 2026). This consideration is directly relevant to Theri landscapes, where transitions between exposed sand, vegetation, agriculture and built-up surfaces can produce heterogeneous thermal pixels. Understanding the relationships between Theri soils and other LULC has practical significance for land-use planning, ecological conservation, agricultural management and climate-resilient development in Theri landscapes. If Theri soils are inherently sensitive to changes in surface moisture and vegetation, then maintaining vegetation cover around and within Theri formations may help moderate extreme surface heating. Similarly, avoiding unnecessary conversion of vegetated or agricultural land into barren surfaces could limit the expansion

of thermally hot areas. Where urban development occurs near Theri landscapes, spatial planning that maintains vegetation buffers and minimizes continuous impervious surfaces may help reduce localized thermal coupling. Such measures are consistent with the broader evidence that vegetation and landscape configuration play important roles in regulating surface thermal environments (Yao et al., 2017; Ziter et al., 2019b).

Therefore, the present study addresses an important gap by investigating the spatio-temporal thermal behaviour of Theri soils and their relationship with adjacent land-use classes using satellite-derived LST. Landsat imagery provides the spatial resolution necessary to distinguish individual land-use environments and to investigate thermal relationships across multiple buffer distances, while the decade-long analysis provides an opportunity to examine both seasonal/interannual variability and persistent spatial associations. In particular, evaluating LST relationships at three concentric zones of 0–1 km, 1–2 km and 2–5 km provides an explicit means of examining whether the thermal association of Theri soil with vegetation, built-up, agricultural and barren land is localised or spatially extensive. Unlike conventional LST–LULC studies that primarily classify thermal differences among land-cover categories, this study evaluates Theri soil as a distinct thermal landscape unit and quantifies its association with neighbouring land-use classes across multiple spatial distances, complemented by field-based surface-temperature observations.

2 Materials and methods

2.1 Study area

The study area, Kuthiraimozhi Theri, is located in the Udangudi Block of Thoothukudi district, Tamil Nadu, India. It forms part of the Theri soil landscape of southern Tamil Nadu, characterized by distinctive red sandy dune deposits locally known as *Theri*. The broader geographical extent of the region ranges from 8°15′0″ N to 9°25′0″ N latitude and 77°05′0″ E to 78°35′0″ E longitude. Theri landscapes are predominantly distributed along the coastal belt of Thoothukudi and Tirunelveli districts, with the largest extent occurring in Thoothukudi district. Earlier soil-survey investigations reported approximately 20,171 ha of Theri soils, of which about 16,978 ha occur in Thoothukudi district. Major Theri belts include Kuthiraimozhi, Thisaiyanvilai, Surangudi, Uvari, Udangudi, Nangaimozhi and Servaikaranmadam. The Kuthiraimozhi Theri forest ecosystem has been protected as a reserve forest by the Department of Forests, Government of Tamil Nadu, since 21 July 1982. The area forms part of a relatively flat alluvial plain, with elevations ranging from 5 to 62 m above mean sea level. Drainage density is low, and the drainage network exhibits a sub-dendritic pattern. The southern branch of the Tamirabarani River and the Karamanayar River occur to the north and south of the study area, respectively.

The climate is humid, with an average annual rainfall of approximately 700 mm, predominantly received during the northeast monsoon from October to December. The soil assemblage is diverse and includes coastal sands and Quaternary alluvial deposits associated with black soils (Udayanapillai and Ganeshamoorthy, 2013). The Theri formations are geomorphologically distinctive red sand dunes developed from sandy deposits and are particularly prominent around Kuthiraimozhi. Geological investigations have described these deposits as containing abundant quartz and feldspar together with accessory heavy minerals such as ilmenite, rutile, garnet, magnetite, hematite, zircon, diopside, hypersthene and biotite (Alagaiah Venu & Velmayil, 2021b). The characteristic reddish colour of the Theri sands has been attributed to leaching, weathering and oxidation processes affecting iron-bearing minerals. The geological framework comprises a Proterozoic basement overlain by Tertiary and Quaternary deposits, including shell limestone and laterite, together with recent black soils, red Theri soils, river alluvium and beach sands (Jayangondaperumal et al., 2012).

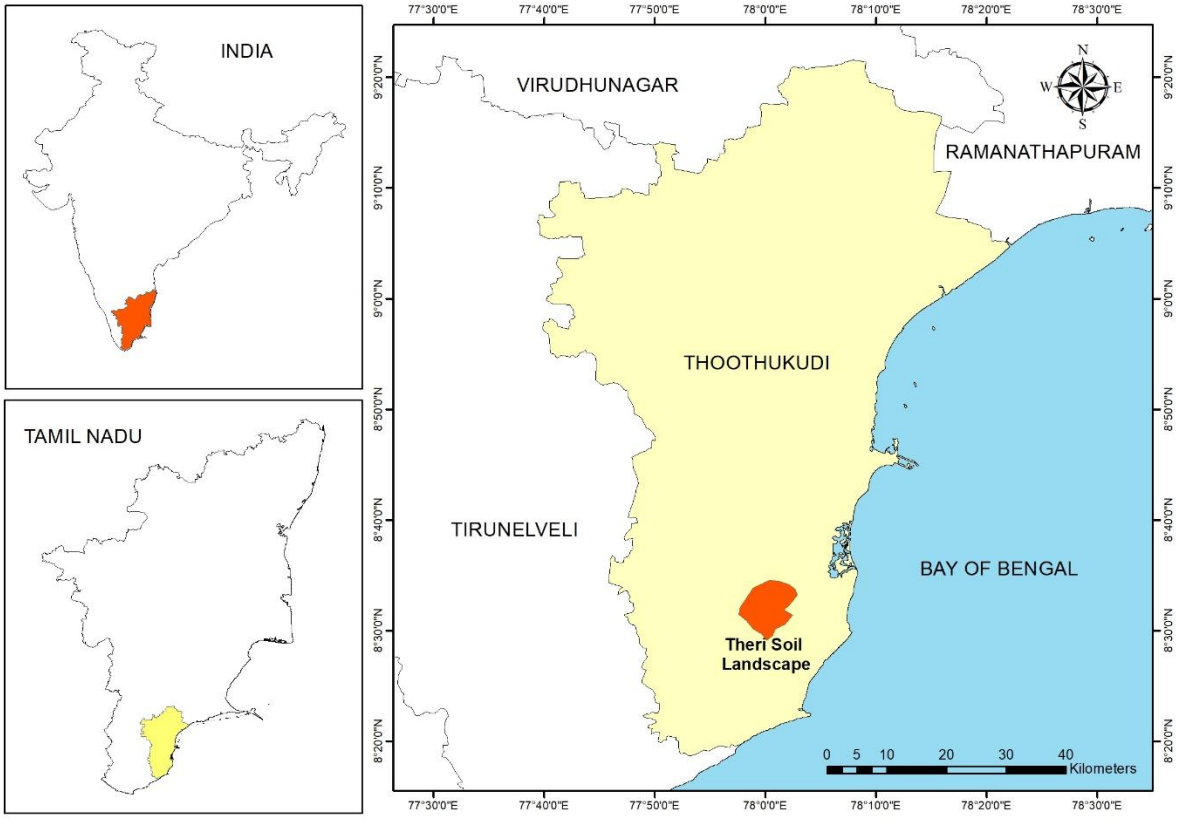


Fig. 1 Theri soil landscape of Thoothukudi, Tamil Nadu

Land use within and around the Theri landscape is heterogeneous, with agriculture occurring alongside natural vegetation, forest patches, settlements, barren surfaces and extensive Theri sand-dune formations. The natural vegetation includes xerophytic species such as *Acacia planifrons*, *Prosopis juliflora*, *Acacia holosericea*, and Acacia melanoxylon, with forested areas also present in the landscape (V. Muneeswaran & M. Udayakumar,

2022). The coexistence of these contrasting land-use and land-cover types provides a suitable setting for examining spatial variations in land surface temperature and the thermal association of Theri soils with neighbouring surfaces. The study area is well connected by national and state highway networks linking Thoothukudi, Tirunelveli and Tiruchendur. The elevated dunes could also be recognised as potential groundwater recharge zones (Carretero et al., 2014). In the present study, the Theri soil landscape (Fig. 1) is therefore considered a thermally sensitive sandy surface, and its LST is evaluated in relation to four major surrounding land-use categories: built-up land, vegetation, agricultural land and barren land, using multiple spatial buffers. This enables assessment of whether the thermal association, or the association of the Theri soil, is localised or extends into the surrounding landscape.

2.2 Computation of land surface temperature

Land Surface Temperature (LST) deals with energy exchange between the Earth's surface and the environment. This study utilizes Landsat 8 satellite data to analyse LST. Specifically, the thermal band (Band 10) data from Landsat 8 is used for LST calculation (Abidin et al., 2021).

The equation for estimation of surface temperature is as follow:

$$T_s = \frac{K_2}{ln\left(\frac{\varepsilon_s * K_1}{\rho_b}\right)}$$

The surface temperature was estimated based on the radiance values calculated from these thermal bands. The spectral radiance (ρ_b) for Band 10 was computed using the digital number (DN_b) of each pixel and the radiometric rescaling factors provided in the image metadata. These constants correspond to Band 10 of the Landsat 8 thermal sensor. Once the radiance is determined, the surface temperature (Ts) is calculated using a standard thermal conversion formula that includes K1 and K2 constants for Band 10, which are 774.8853 and 1321.0789 respectively, as per the metadata file. The radiance was calculated using the following equation:

$$\rho_b = Add_{rad,b} + \left(Mult_{rad,b} * DN_b\right)$$

Where $Add_{rad,b}$ and $Mult_{rad,b}$ are the additive and multiplicative rescaling factors used to convert digital numbers (DN) into spectral radiance for each band. The values of Add_{rad} and $Mult_{rad}$ for band 10 are 0.10000 and 3.3420E-04, respectively.

220 Surface Emissivity (ε_s) is defined as the ratio of thermal energy emitted by a real surface to that emitted
221 by a perfect blackbody at the same temperature, and it was estimated to account for the land surface's ability to
222 emit thermal radiation compared to a perfect blackbody.

223 $$\varepsilon_s = \begin{cases} 1.009 + 0.047(ln(NDVI)) \rightarrow (NDVI > 0) \\ 1 \rightarrow (NDVI < 0) \end{cases}$$

224 It was derived empirically using NDVI-based methods. NDVI (Normalized Difference Vegetation Index)
225 was calculated using the following formula (Tucker, 1979):

226 $$NDVI = \frac{NIR - RED}{NIR + RED}$$

227 Surface emissivity values were then adjusted based on NDVI thresholds, as different land covers (e.g.,
228 vegetation, soil, urban areas) exhibit different emissivity characteristics.

229 *2.3 Data sources, period and LST computation*

230 Landsat 8 satellite imagery was used to assess the spatio-temporal variation of LST over the Theri soil
231 landscape and its surrounding land-use classes during 2015–2024. The analysis was implemented in the Google
232 Earth Engine (GEE) cloud-computing platform, which enabled systematic processing of the multi-temporal
233 satellite observations. The derived LST was then extracted for Theri soil and the surrounding built-up, vegetation,
234 agricultural and barren land-use classes at three concentric zones of 0–1 km, 1–2 km and 2–5 km from the Theri
235 soil boundary. The resulting multi-temporal LST datasets were used for comparative analysis, correlation and
236 pairwise scatter analysis to evaluate the strength and spatial dependence of thermal relationships between Theri
237 soil and the adjacent land-use classes. The overall workflow adopted for LST estimation using GEE is presented
238 in Fig. 2.

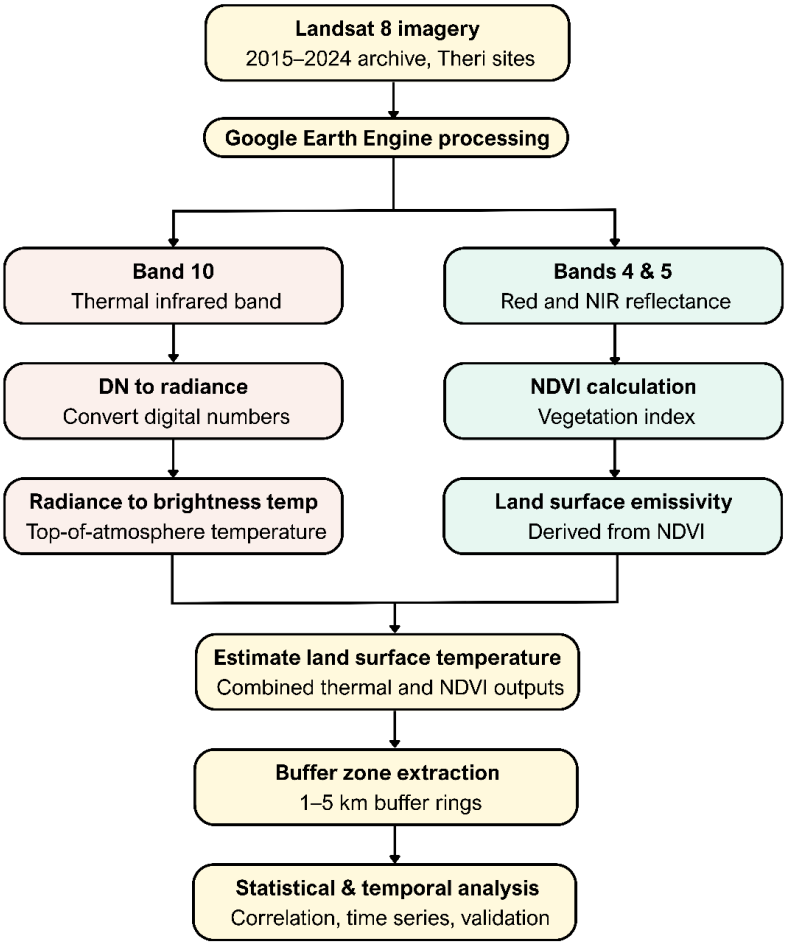


Fig. 2 Flowchart LST Estimation using Google Earth Engine

2.4 Ground truth verification of LST

Ground truth observations were carried out to assess the reliability of the satellite-derived LST values over the Theri soil landscape (Fig. 3). Field measurements were obtained using a handheld infrared thermometer at representative locations covering the major surface conditions considered in the study, including Theri soil, vegetation, agricultural land, built-up surfaces and barren land. The geographic coordinates of the observation locations were recorded, and the measured temperature values were subsequently compared with the corresponding Landsat-derived LST values. To corroborate the satellite-derived LST patterns above, field-based surface-temperature observations were collected across six sites (Nalumavadi, Kayamozhi, Angamangalam, Kuthiraimozhi, and Thoothukudi), each visually classified into a land-use/landscape type. For comparability with the satellite land-use scheme, were consolidated into six categories: Theri Soil (Open/Exposed), Theri Soil (Vegetated), Barren Land, Built-up, Vegetation, and Agriculture. The comparison was used to evaluate the agreement between field observations and remotely sensed LST and to provide an independent ground reference for the satellite-based temperature estimates.

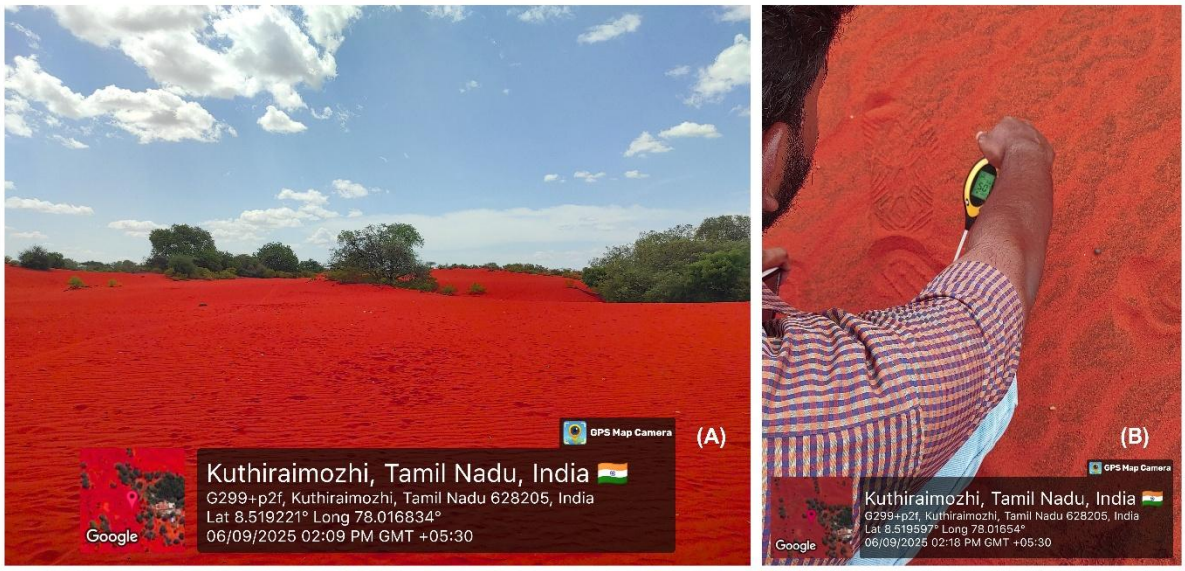


Fig. 3 Field observations of Theri soil surface temperature at Kuthiraimozhi, Tamil Nadu: (A) red sand dune landscape and (B) in situ temperature measurement of the exposed Theri sand surface

3 Results

3.1 Temporal variability of LST across Theri soil and surrounding land-use classes

The temporal variation in LST of Theri soil and the surrounding land-use classes was examined for the period 2015–2024. The time-series plots revealed substantial temporal variability across all land-use categories, with recurrent periods of simultaneous increases and decreases in LST (Figs. 4-7). Despite differences in the magnitude of surface temperature among land-use classes, the major temporal fluctuations were broadly synchronous, indicating a common regional thermal forcing. Theri soil generally exhibited the highest LST throughout the observation period. The Theri soil LST frequently reached approximately 40–45 °C, particularly during several high-temperature episodes, whereas vegetation, agricultural and, in most cases, built-up surfaces exhibited lower temperatures. Several pronounced reductions in LST occurred simultaneously across Theri soil and surrounding land uses, demonstrating that the thermal behaviour of the different surfaces was not independent.

3.1.1 Theri soil and vegetation

The temporal profiles of Theri soil and vegetation showed a clear correspondence throughout the study period (Fig. 4). Although Theri soil generally maintained higher LST, vegetation within the Theri landscape and vegetation at 1 and 2 km followed the major temporal fluctuations of Theri soil. The correlation matrix showed a strong positive relationship between Theri soil and vegetation within the Theri landscape ($r = 0.89$). The correlations remained strong at 1 and 2 km, with $r = 0.83$ for both distances (Fig. 8). Thus, the strength of the association declined with increasing distance from 0 to 1 km but remained substantial at 2 km. The pairwise scatter

plots supported these findings, showing a distinct positive and approximately linear distribution of observations (Fig. 9). Vegetation within the Theri landscape exhibited relatively compact clustering around the increasing trend, whereas vegetation at 1 and 2 km showed somewhat greater dispersion, particularly at lower LST values. This indicates that vegetation retained strong temporal thermal synchrony with Theri soil but exhibited greater variability in its surface thermal response.

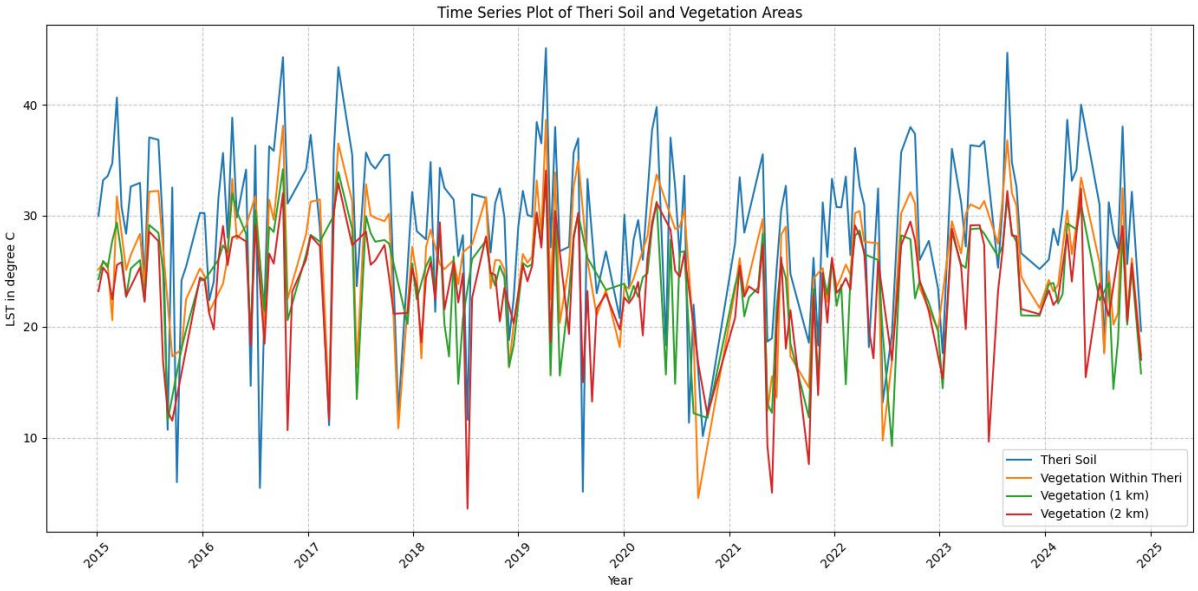


Fig. 4 Time series plot of Theri Soil and Vegetation

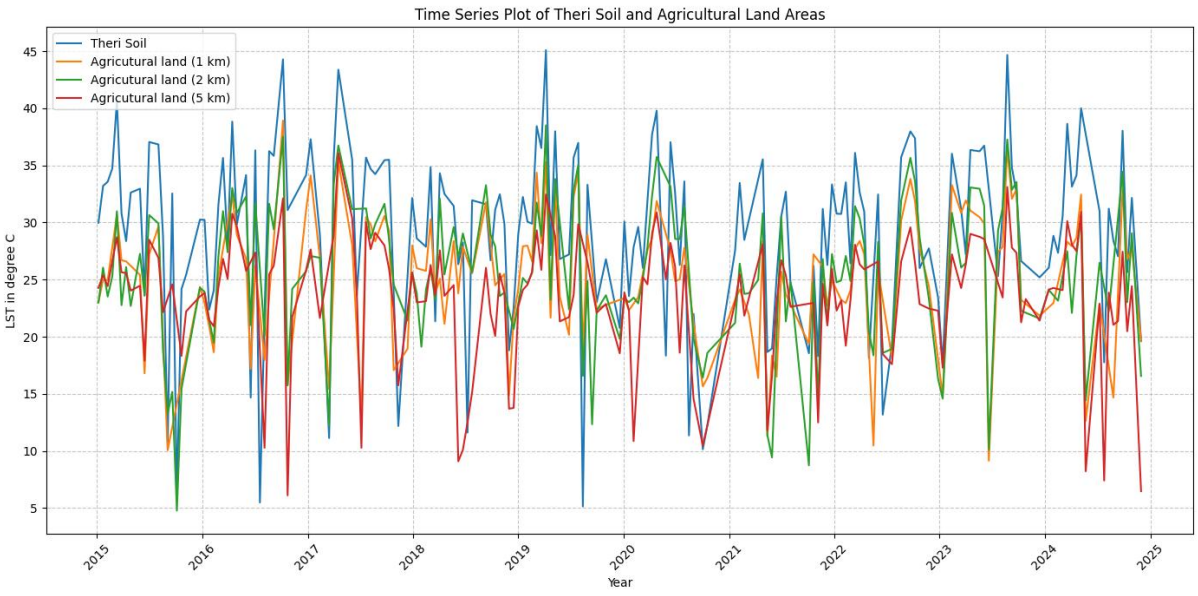


Fig. 5 Time series plot of Theri Soil and Agricultural Land

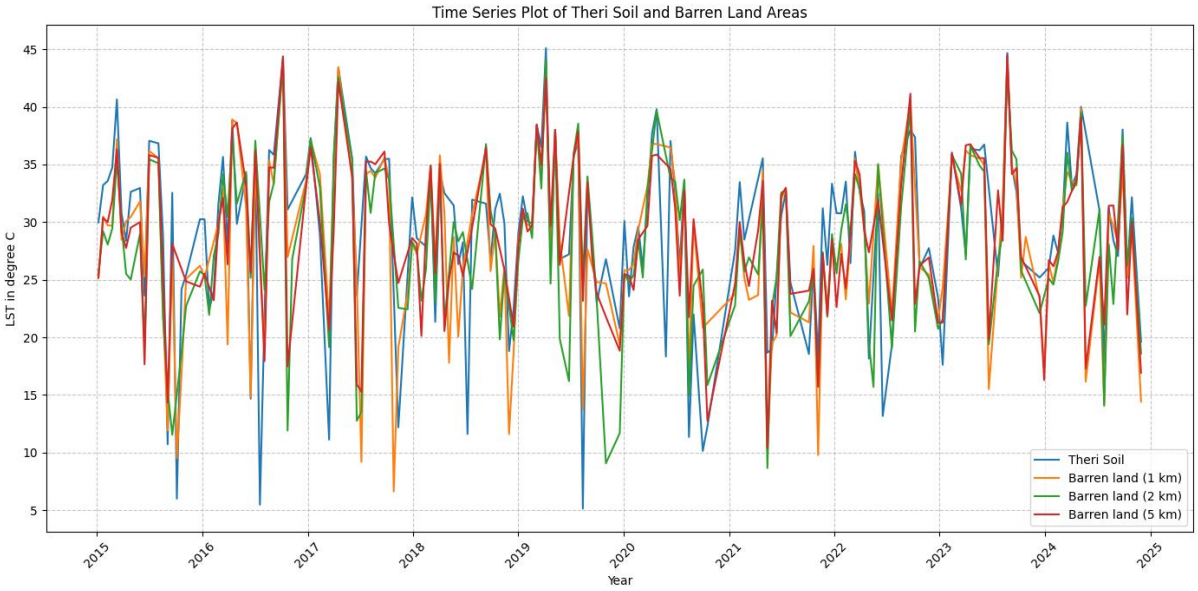


Fig. 6 Time series plot of Theri Soil and Barren Land

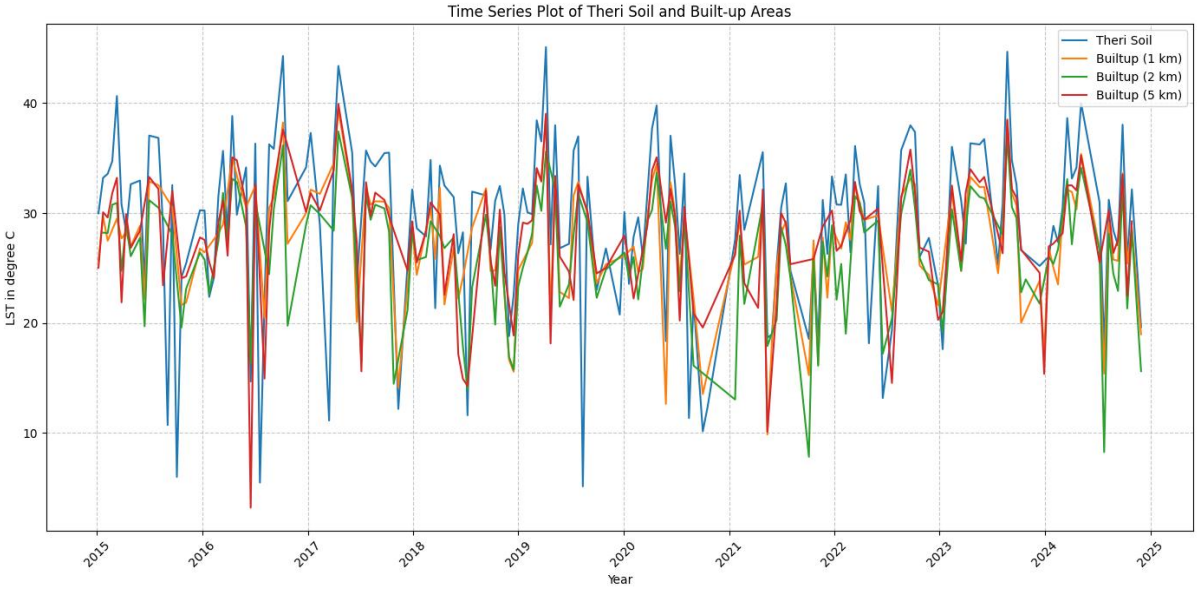
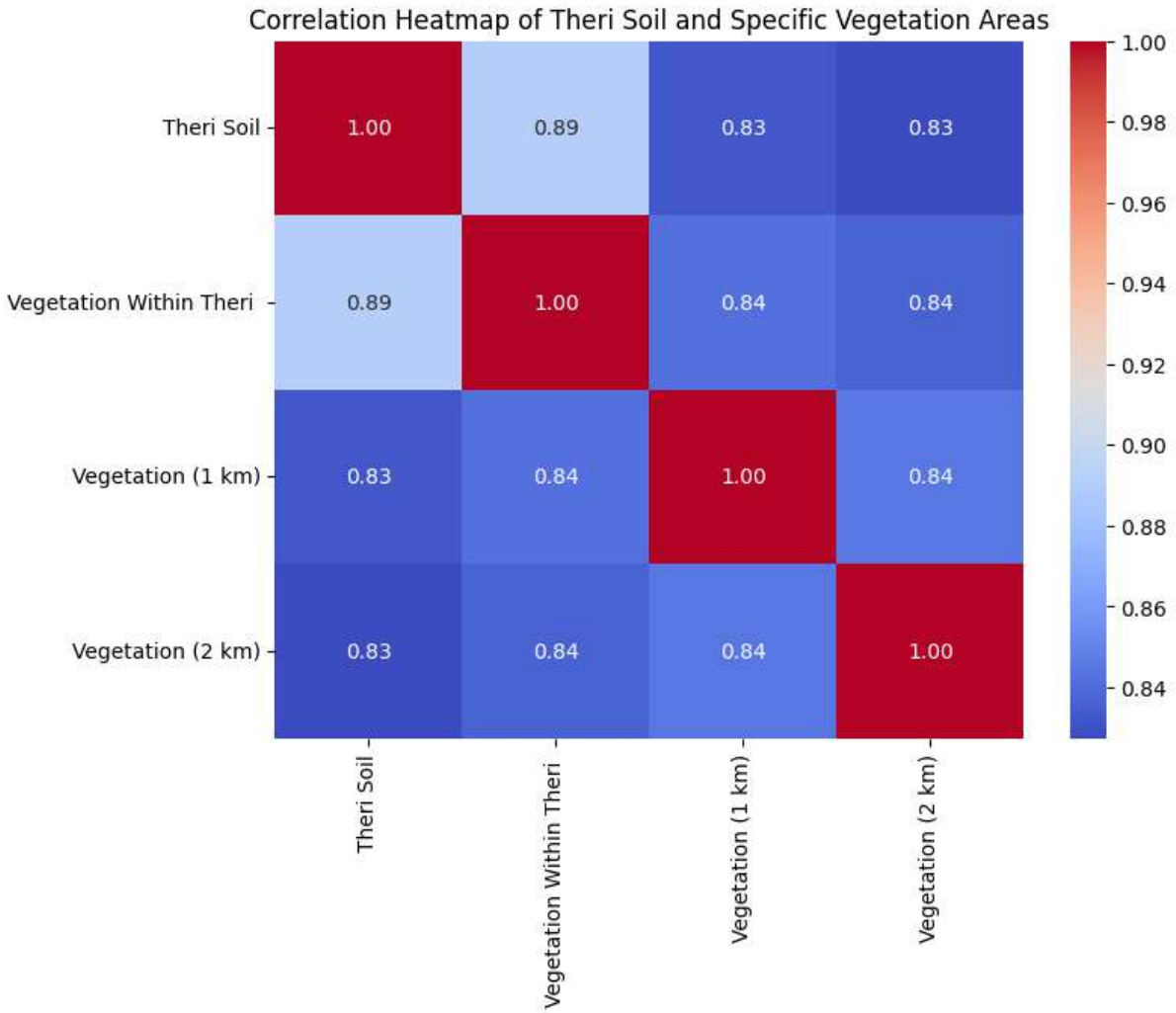


Fig. 7 Time series plot of Theri Soil and Built-up



289

290 **Fig. 8** Correlation matrix of Theri Soil and Vegetation

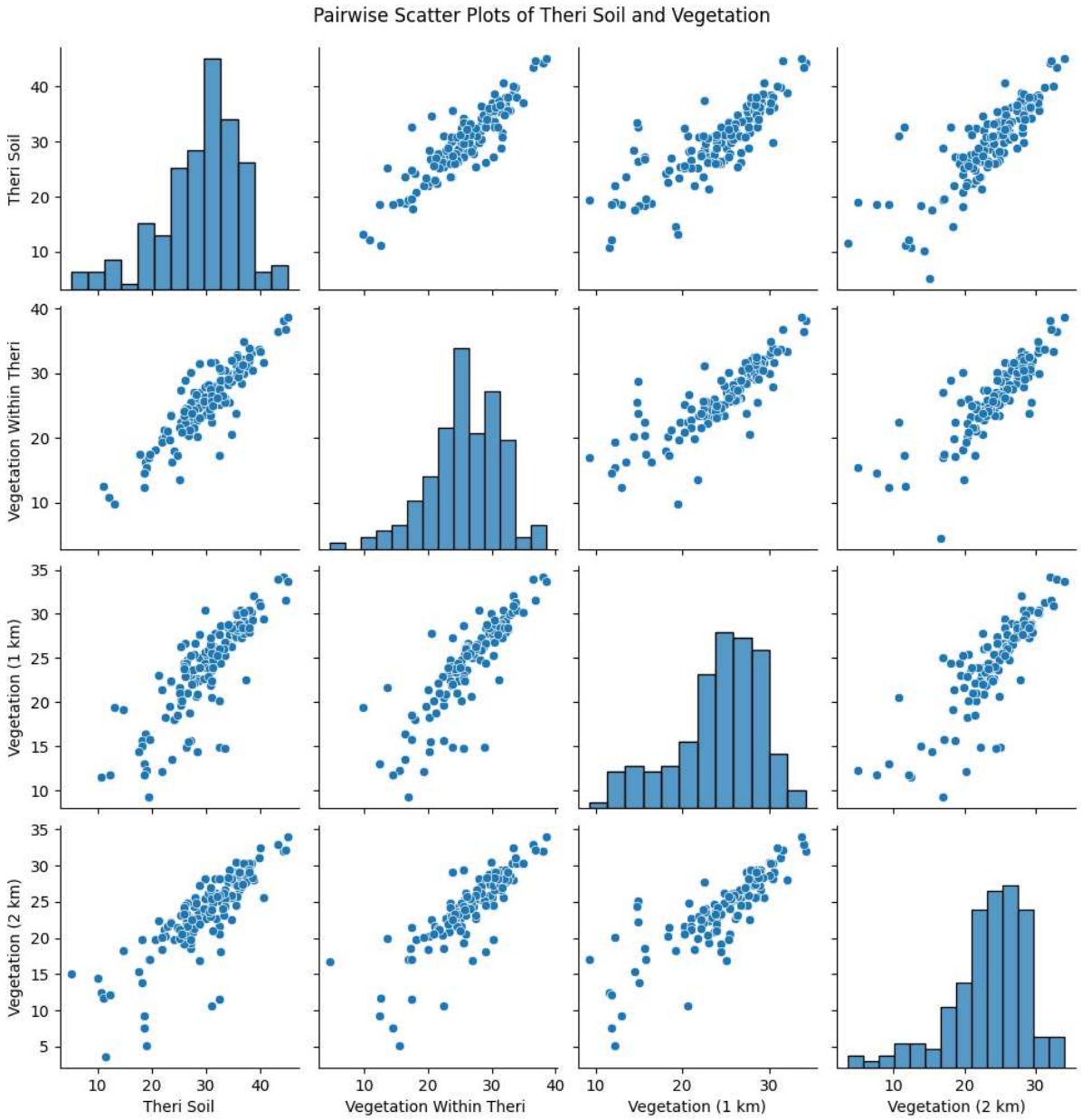


Fig. 9 Pairwise scatter plots of Theri Soil and Vegetation

3.1.2 Theri soil and agricultural land

Agricultural surfaces also exhibited strong temporal correspondence with Theri soil (Fig. 10). Theri soil generally recorded higher LST than agricultural land, particularly during high-temperature periods. Agricultural land at 1 and 2 km showed broadly similar temporal fluctuations, while the 5-km agricultural area exhibited comparatively greater variability. The correlation coefficients between Theri soil and agricultural land were 0.83 at 1 km, 0.83 at 2 km and 0.78 at 5 km. Thus, the association was strongest within the immediate 1–2 km surroundings and declined at the 5-km scale. The corresponding pairwise scatter plots (Fig. 11) displayed strong

positive relationships, although the agricultural observations were more widely dispersed than those of built-up land. The greater dispersion was particularly evident at 5 km, where several observations deviated from the principal linear trend. This suggests that agricultural LST is influenced not only by regional thermal conditions but also by spatially variable surface conditions.

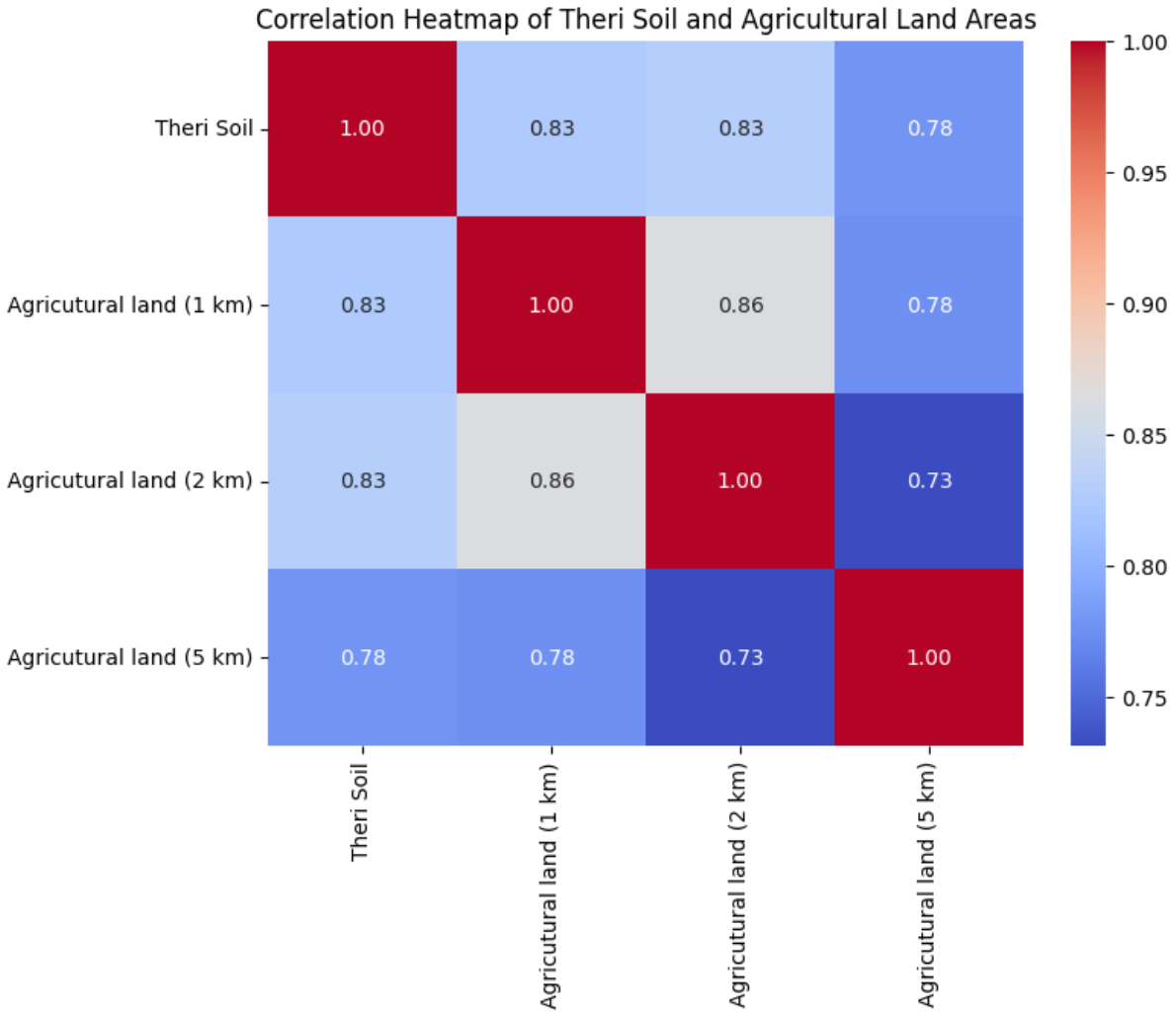


Fig. 10 Correlation matrix of Theri Soil and Agricultural Land

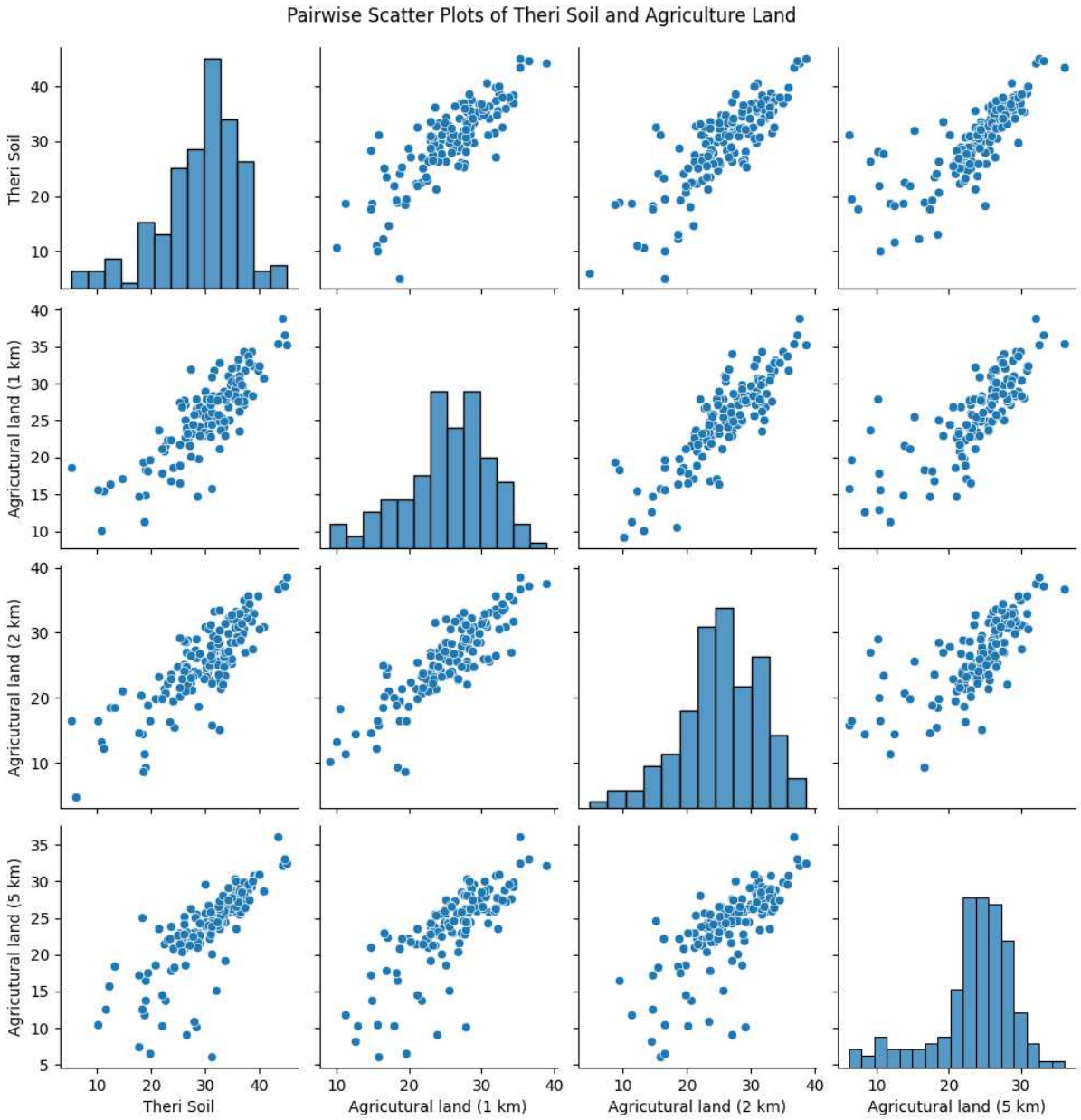


Fig. 11 Pairwise scatter plots of Theri Soil and Agricultural Land

3.1.3 Theri soil and barren land

Barren land showed a strong temporal resemblance to Theri soil (Fig. 12). The major high- and low-temperature episodes observed in Theri soil were generally reproduced by barren surfaces at the three investigated distances. In several high-LST periods, barren land approached the LST values observed for Theri soil. The correlation coefficients were 0.87, 0.76 and 0.79 for barren land at 1, 2 and 5 km, respectively. The strongest relationship therefore occurred at 1 km, while the relationship weakened at 2 km before showing a slight increase at 5 km. The pairwise scatter plots showed pronounced positive relationships at all three distances (Fig. 13). The 1-km observations were relatively tightly clustered around the principal trend, whereas the 2-km observations

exhibited greater dispersion and several deviations from the dominant relationship. The 5-km observations again demonstrated a strong positive association.

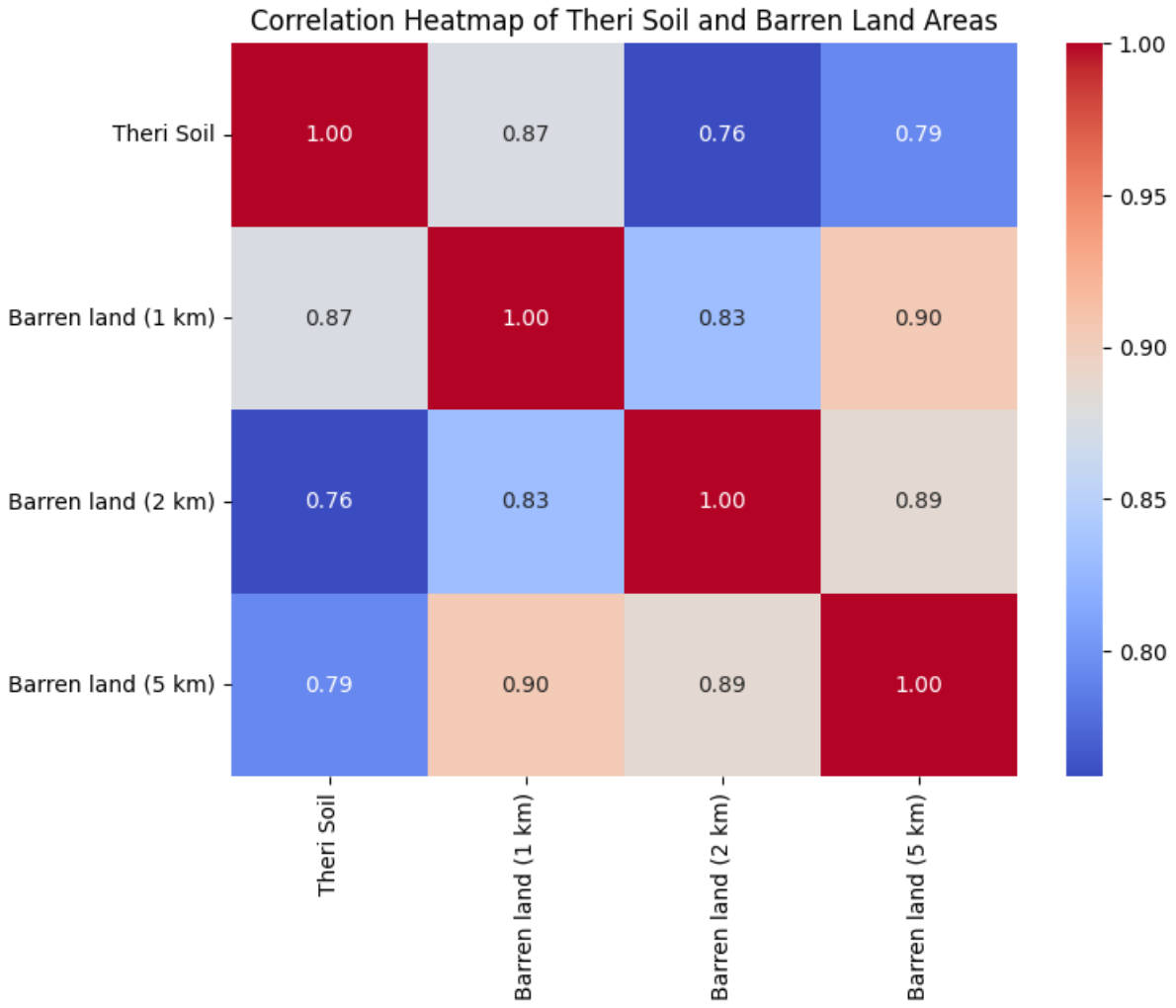


Fig. 12 Correlation matrix of Theri Soil and Barren Land

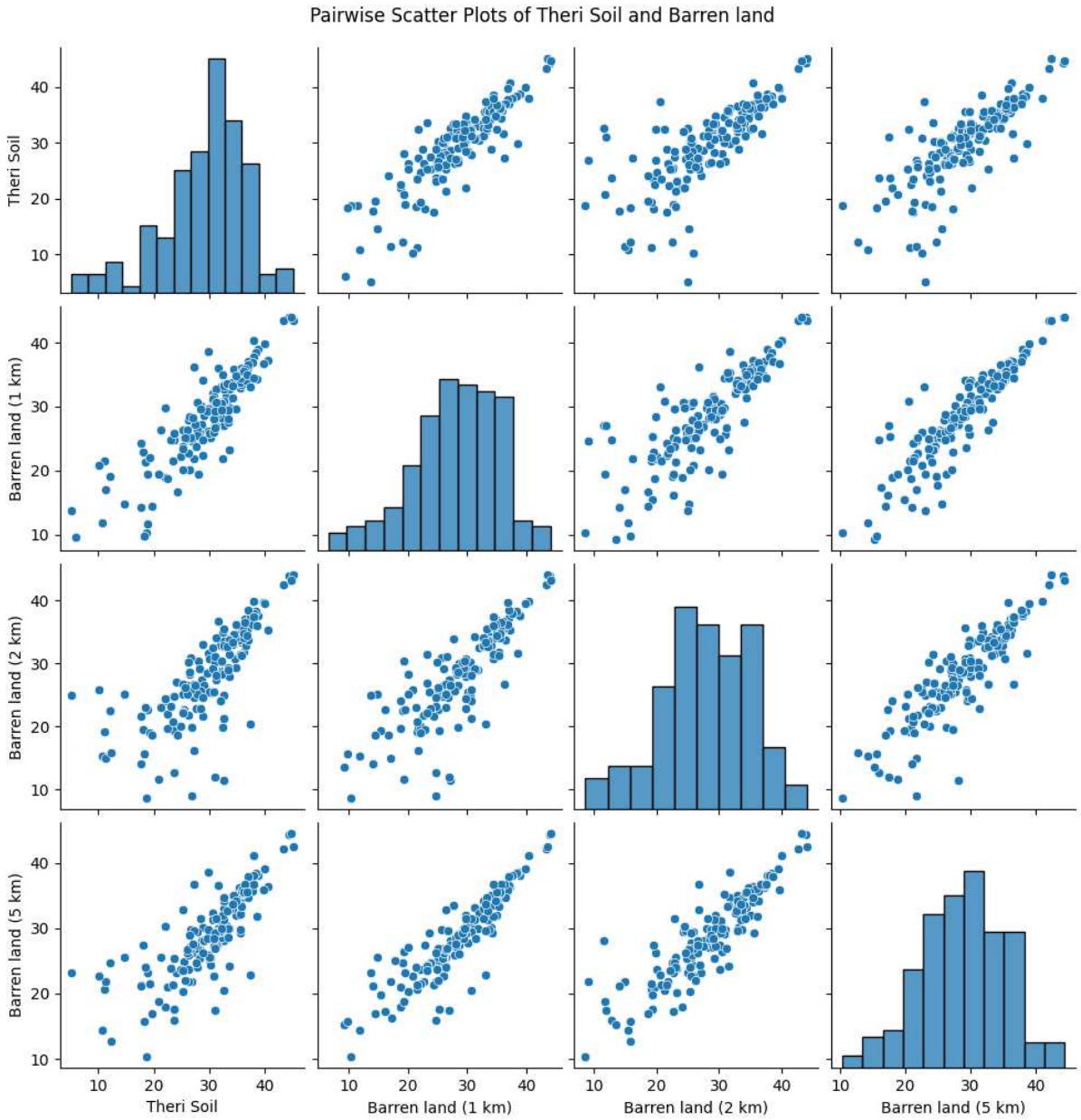


Fig. 13 Pairwise scatter plots of Theri Soil and Barren Land

3.1.4 Theri soil and built-up areas

Among all land-use classes, built-up land at 1 km exhibited the strongest correlation with Theri soil. The correlation coefficients between Theri soil and built-up land were 0.92 at 1 km, 0.85 at 2 km and 0.82 at 5 km (Fig. 14). The pairwise scatter plot for the 1-km built-up area showed a particularly compact linear distribution, indicating strong thermal synchrony between nearby built-up surfaces and Theri soil (Fig. 15). The scatter increased progressively at 2 and 5 km, although the positive relationship remained evident. The time series similarly demonstrated that major increases and decreases in Theri soil LST were generally accompanied by

corresponding changes in built-up LST. However, built-up surfaces generally remained below the highest Theri soil temperatures.

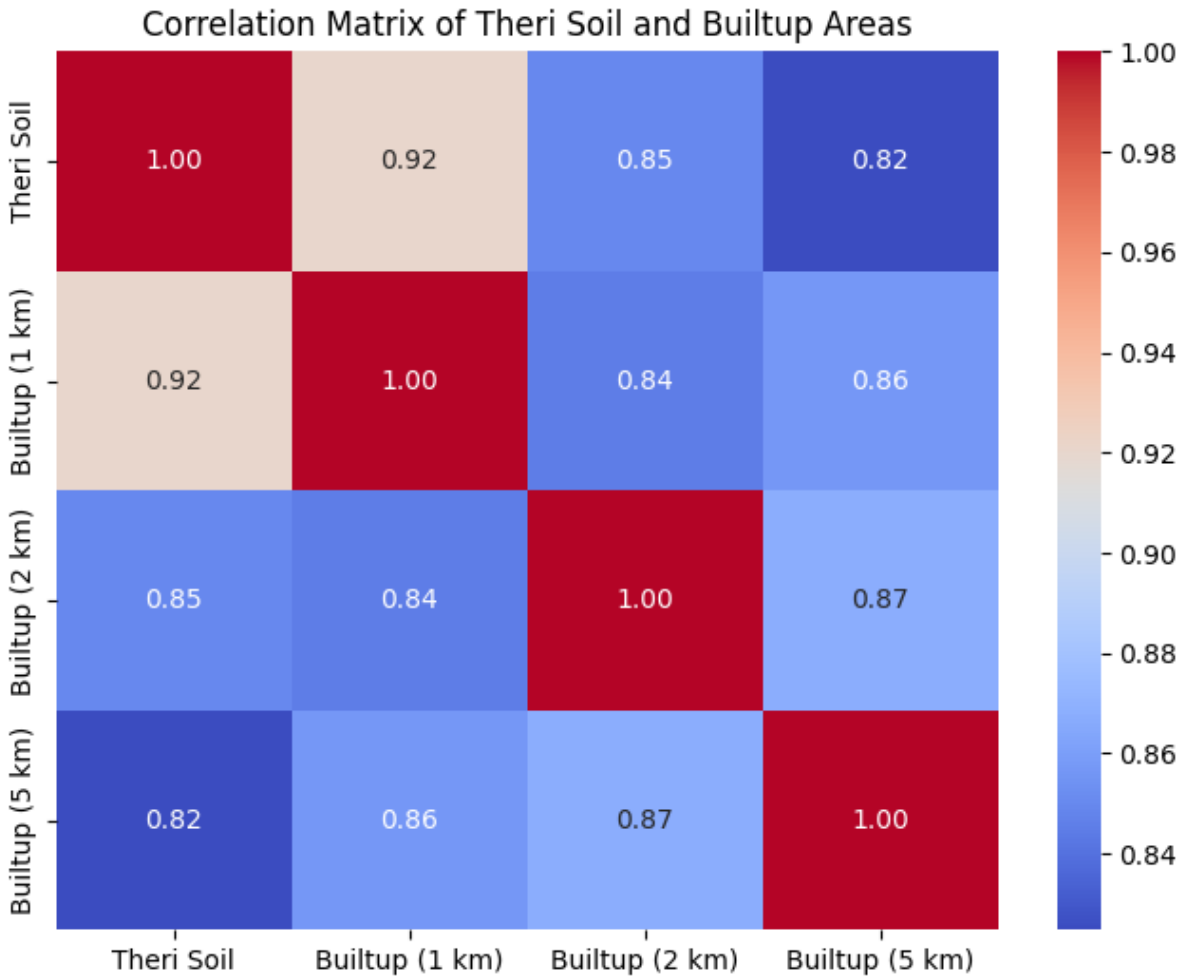
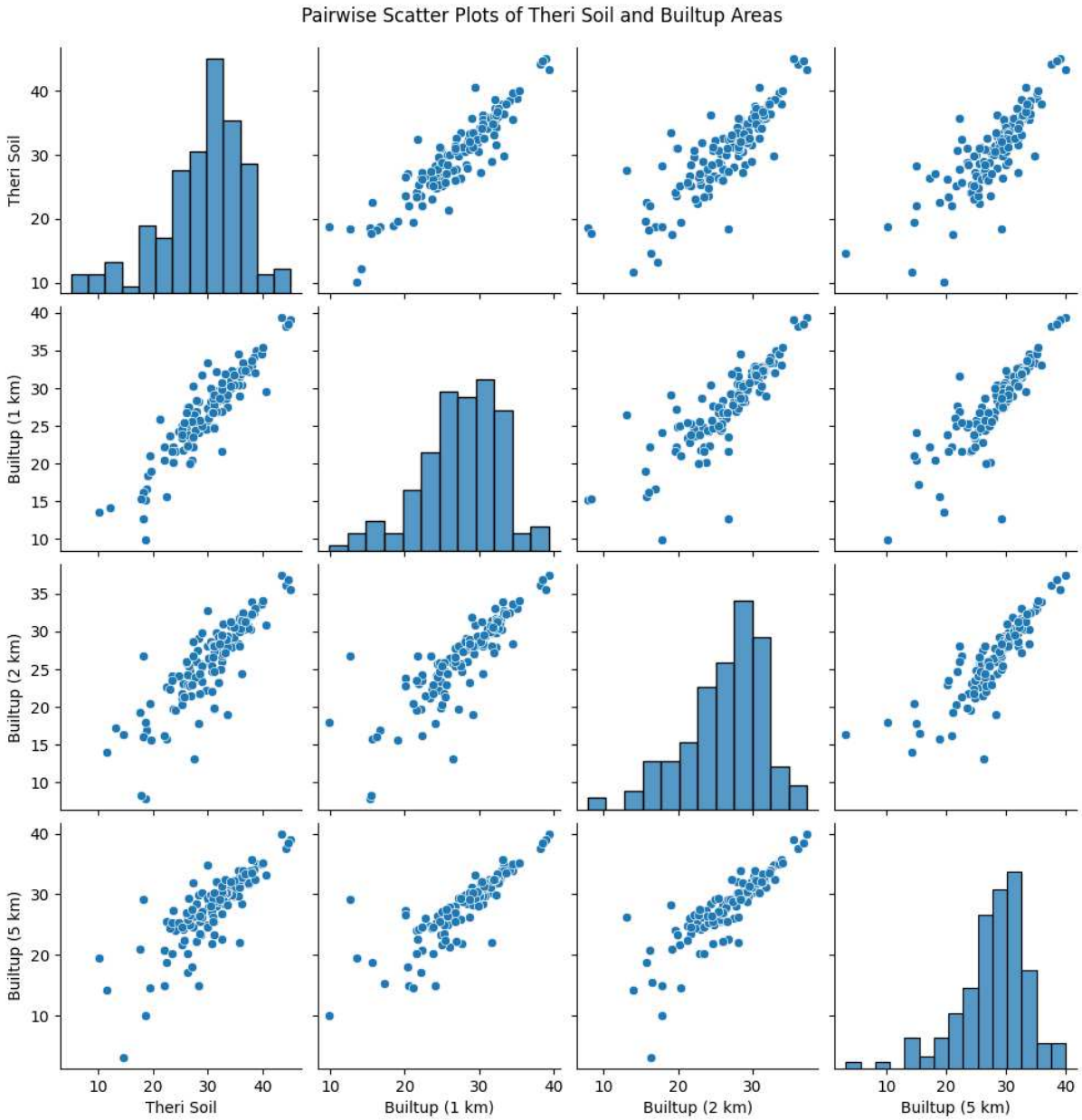


Fig. 14 Correlation matrix of Theri Soil and Built-up Areas



334

335 **Fig. 15** Pairwise scatter plots of Theri Soil and Built-up Areas

336 *3.2 Correlation structure among land-use classes*

337 The correlation matrices demonstrated that the thermal relationships extended beyond the Theri soil–
338 land-use pairs to include relationships among the surrounding land-use classes themselves. For built-up areas, the
339 correlations among the 1-, 2- and 5-km zones were 0.84–0.87, indicating strong consistency in the temporal
340 thermal behaviour of built-up surfaces across spatial scales. Similarly, vegetation at different distances showed
341 strong interrelationships, with coefficients of approximately 0.84. Agricultural land exhibited correlations of 0.86
342 between 1 and 2 km, while the relationship between the 2- and 5-km zones was comparatively lower (r = 0.73).
343 This indicates increasing spatial variability in agricultural LST at larger distances. Barren land exhibited strong

inter-zone correlations, ranging from 0.83 to 0.90, demonstrating considerable temporal consistency among barren surfaces. The relatively high correlations among different buffer zones indicate that the temporal thermal behaviour of each land-use class is influenced by a common regional signal.

3.3 Ground-Truth (In-Situ) validation

Field measurements confirmed the thermal hierarchy observed from the Landsat LST analysis: open Theri soil (55.6 °C) > barren land (45.0 °C) > built-up (43.0 °C) > vegetated Theri soil (40.2 °C) > vegetation (35.8 °C) > agriculture (35.0 °C). The maximum recorded temperature was 57.3 °C for open Theri soil, whereas agriculture recorded the lowest value (35.2 °C). The strong agreement between handheld measurements and Landsat-derived LST ($R^2 = 0.791$) indicates good correspondence and supports the reliability of the satellite-based LST estimates (Fig. 16).

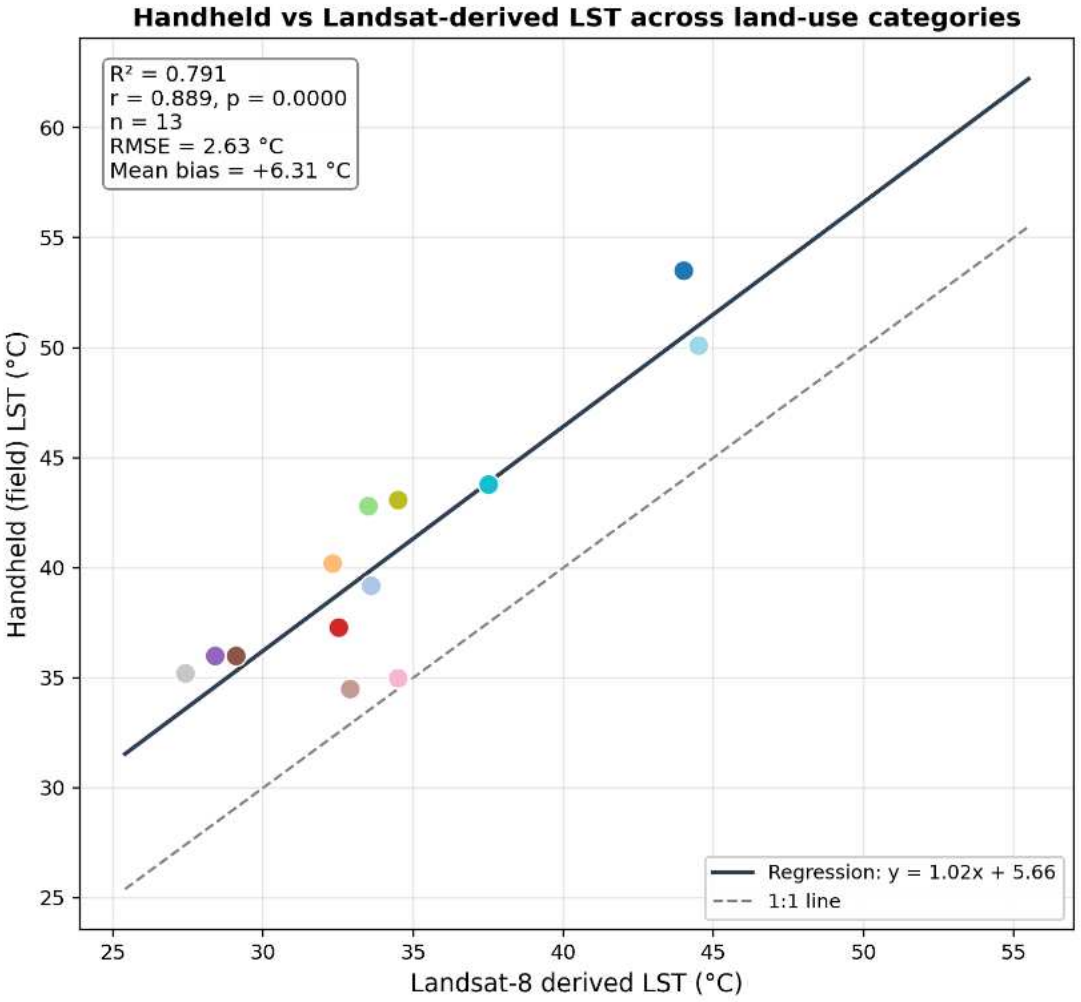


Fig. 16 Field Validation of Satellite-Derived LST

4 Discussion

The combined temporal series, correlation matrices and pairwise scatter plots indicate that the Theri soil landscape is a thermally interconnected system in which neighbouring land-use classes share a strong temporal signal, although they differ in absolute surface temperature. Across 2015–2024, Theri soil generally recorded the highest satellite-derived LST and frequently reached about 40–45 °C, while vegetation and agriculture were usually cooler and barren and built-up surfaces showed relatively higher values. The repeated coincidence of LST peaks and troughs indicates that regional meteorological forcing is a major control on temporal variability. This agrees with the established basis of thermal remote sensing, in which surface radiation and energy exchange determine LST while heterogeneous land surfaces modify the partitioning of available energy (Roy & Bari, 2022; Sobrino et al., 2020). Accordingly, the strong correlations observed here indicate thermal synchrony rather than direct causal influence among land-use classes. The pronounced seasonal and interannual variability should also not be interpreted as a statistically significant long-term warming or cooling trend because formal trend tests were not undertaken.

The strongest association occurred between Theri soil and built-up land, with $r = 0.92$ at 1 km, decreasing to 0.85 at 2 km and 0.82 at 5 km. The compact 1-km scatter relationship and increasing dispersion with distance indicate stronger short-range thermal coherence. Built-up surfaces commonly have limited evapotranspiration and appreciable heat storage, influencing their surface energy balance and LST (Voogt & Oke, 2003; Wang et al., 2023). Globally, artificial impervious surface fraction is generally positively related to LST, while vegetation and albedo modify the magnitude of this relationship, showing that built-up thermal behaviour is governed by interacting surface properties rather than imperviousness alone (Q. Yang et al., 2021). Multi-scale analyses further demonstrate that landscape composition and configuration influence LST relationships differently as neighbourhood extent changes (Wu et al., 2022). These mechanisms help explain why the nearby 1-km built-up zone was most closely synchronized with Theri soil, whereas more heterogeneous land-use mixtures at 2 and 5 km weakened the association. The result does not demonstrate that built-up land directly heats Theri soil; shared meteorological forcing and similarly limited evaporative buffering provide the more defensible interpretation. Vegetation showed a strong but physically different response. The correlation between Theri soil and vegetation within the Theri landscape was $r = 0.89$, while vegetation at 1 and 2 km remained strongly associated at $r = 0.83$. Nevertheless, vegetation consistently remained cooler than Theri soil. This contrast is important because correlation describes the timing of thermal fluctuations, whereas the lower LST of vegetation reflects differences in thermal magnitude. Vegetation can reduce surface heating through shading and enhanced latent heat flux

associated with evapotranspiration. Long-term remote-sensing evidence shows that vegetation growth generally produces negative feedback on LST in many land-cover settings, although the strength of cooling varies with background climate and surface conditions (Xue et al., 2021). In subtropical landscapes, vegetation has also been shown to reduce daytime LST, with the cooling response depending on vegetation condition and landscape context (S. Zhou et al., 2023). Thus, vegetation around Theri appears to moderate heating while remaining temporally coupled to the same regional forcing.

Agricultural land exhibited positive associations with Theri soil at 1 km ($r = 0.83$), 2 km ($r = 0.83$) and 5 km ($r = 0.78$), with greater scatter at the larger distance. This pattern suggests persistence of the regional thermal signal together with increasing local variability. Crop phenology, irrigation, soil moisture and harvesting alter the surface energy balance and can change LST through time. Comparative observations in eastern China showed that agriculture can cool the surface relative to surrounding conditions, whereas urbanization tends to warm it; these effects depend strongly on vegetation activity, evapotranspiration, albedo and background climate (D. Zhou et al., 2016). Thermal remote sensing at field scale similarly demonstrates the sensitivity of crop water status and evaporative stress to LST dynamics (Y. Yang et al., 2018). The modest decline from 0.83 to 0.78 at 5 km is therefore consistent with increasing agricultural heterogeneity rather than disappearance of the regional thermal control.

Barren land showed a strong resemblance to exposed Theri soil, with correlations of 0.87 at 1 km, 0.76 at 2 km and 0.79 at 5 km. This similarity is physically plausible because both surfaces have limited vegetation-mediated cooling and are directly exposed to solar radiation. Dry exposed surfaces can develop high LST, while moisture and thermal properties modify the response under different terrain conditions (Asadzadeh & Souza Filho, 2023). The non-monotonic 0.87–0.76–0.79 sequence is therefore important because it shows that thermal association need not decline smoothly with distance. Differences in moisture, texture, surface roughness and sparse vegetation among barren patches are plausible explanations, although these variables were not directly measured. Landscape studies show that the scale used to characterize composition and spatial arrangement can substantially alter the observed LST relationship (Alexander, 2021). The inter-buffer correlations provide additional evidence for regional thermal coherence. Built-up areas showed correlations of 0.84–0.87 across the 1-, 2- and 5-km zones, vegetation remained near 0.84, and barren land showed 0.83–0.90. Agriculture was less spatially coherent, including $r = 0.73$ between the 2- and 5-km zones. This indicates that thermal variability retains a common regional component across kilometre-scale areas, while local land-surface characteristics introduce class-specific heterogeneity. Such scale dependence is consistent with multi-resolution LST studies showing that both spatial

grain and extent influence the strength of relationships between land-surface pattern and temperature (Weng et al., 2004). The distinction between shared temporal forcing and land-use-specific thermal magnitude is therefore central to interpreting the Theri landscape.

Field observations independently reproduced the broad thermal hierarchy: open Theri soil (55.6 °C) > barren land (45.0 °C) > built-up (43.0 °C) > vegetated Theri soil (40.2 °C) > vegetation (35.8 °C) > agriculture (35.0 °C). The maximum field temperature was 57.3 °C on exposed Theri soil. Handheld observations showed reasonable correspondence with Landsat-derived LST (R^2 = 0.791; r = 0.889; n = 13; RMSE = 2.63 °C). This supports the interpretation that the satellite analysis captured the major thermal contrasts among landscape conditions. However, point-based field measurements and satellite pixels differ in spatial support, observation time and surface representativeness, and mixed surfaces can contribute to discrepancies; therefore, the comparison is best regarded as supporting agreement rather than definitive validation (Morgese et al., 2025).

Overall, Theri soil is a distinct thermal unit embedded within a broader land-use mosaic. The particularly strong 1-km built-up relationship, persistent vegetation cooling, increasing agricultural variability with distance and non-monotonic barren-land response demonstrate that its thermal behaviour results from the interaction of regional forcing with local surface properties. This interpretation is consistent with systematic evidence that LULC–LST relationships vary with land-cover type, spatial context and surface characteristics (Patel et al., 2024). The significance of the present study therefore lies not simply in showing that Theri surfaces are hot, but in demonstrating that their thermal trajectory is strongly connected to the surrounding landscape while the magnitude of heating is regulated by land-use-specific processes.

5 Conclusion

The present study provides a multi-temporal assessment of the thermal behaviour of Theri soil and its surrounding land-use classes using satellite-derived LST, spatial buffer analysis, correlation matrices, pairwise scatter plots and time-series evaluation. The results demonstrate that the Theri landscape exhibits substantial temporal variability in surface temperature, with recurrent periods of elevated and reduced LST throughout the 2015–2024 study period. Despite differences in absolute temperature, the major temporal fluctuations of Theri soil were generally reproduced across the surrounding land-use classes, indicating strong regional thermal coupling. A clear distinction was observed between exposed Theri soil and vegetated and agricultural surfaces. Vegetation generally exhibited lower LST than Theri soil, consistent with the cooling effects of evapotranspiration, canopy shading and greater surface moisture availability. Nevertheless, vegetation showed a

strong temporal correlation with Theri soil, particularly within the Theri landscape (r = 0.89). This demonstrates that high temporal correlation does not necessarily indicate similar thermal magnitude; rather, different surfaces can respond synchronously to common climatic forcing while maintaining distinct surface-temperature regimes. Built-up land showed the strongest short-range thermal association with Theri soil, with correlations of 0.92, 0.85 and 0.82 at 1, 2 and 5 km, respectively. The progressive reduction in correlation with distance suggests that spatial proximity contributes to the degree of thermal synchronisation between Theri soil and built-up surfaces. However, these correlations should not be interpreted as evidence of a direct causal influence of built-up development on Theri soil temperature, because both surfaces are simultaneously affected by regional meteorological forcing. Agricultural land exhibited strong associations at 1 and 2 km (r = 0.83) but a comparatively lower relationship at 5 km (r = 0.78). This spatial variation is likely associated with the influence of crop phenology, irrigation, soil moisture and agricultural management on surface temperature. Barren land demonstrated a particularly strong relationship with Theri soil at 1 km (r = 0.87), reflecting the similarity in thermal response between exposed mineral surfaces with limited vegetation-mediated cooling. However, the lower correlation at 2 km (r = 0.76) and subsequent increase at 5 km (r = 0.79) indicate that thermal association with barren land is influenced by spatial heterogeneity rather than following a simple distance-decay relationship. The pairwise scatter plots further confirmed predominantly positive and approximately linear relationships between Theri soil and the surrounding land-use classes. The strong associations among different buffer zones within the same land-use category indicate that regional climatic forcing is an important control on LST variability, while the differences in correlation strength demonstrate the additional influence of local surface characteristics. The time-series analysis similarly showed that major warming and cooling episodes were frequently shared among land-use classes, confirming the presence of a coherent regional thermal signal. Overall, the findings indicate that Theri soil functions as an important component of the regional surface thermal environment, while surrounding land-use types modify the magnitude and spatial expression of LST. The results emphasise the importance of maintaining vegetation cover and carefully managing land-use transitions around thermally sensitive Theri landscapes. In particular, uncontrolled expansion of impervious surfaces and degradation of vegetated areas could alter surface-energy exchanges and potentially intensify local thermal stress. Conversely, conservation of vegetation and appropriate land-use planning can contribute to thermal regulation and landscape resilience.

Competing Interests:

The authors declare that they have no competing interests that could have influenced the work reported in this manuscript.

Funding

No specific funding was received for this research.

Author Contributions

A.A.R. contributed to conceptualization, methodology, data collection, data analysis, visualization, investigation, and manuscript preparation.

J.R. contributed to methodology, data analysis, visualization, investigation, and manuscript preparation.

Both authors reviewed and approved the final manuscript.

Data Availability

The satellite datasets used in this study are publicly available through the Landsat archive in Google Earth Engine. The processed datasets generated during the study are available from the corresponding author on reasonable request.

Ethics, Consent to Participate, and Consent to Publish

Ethics, Consent to Participate, and Consent to Publish declarations: not applicable.

Acknowledgements

The authors express their sincere gratitude to God Almighty for His grace, guidance, and strength throughout this research. The authors also acknowledge the Department of Environmental Sciences, Tamil Nadu Agricultural University, Coimbatore, for providing academic and research support.

REFERENCES

Abidin, M. R., Nur, R., Mayzarah, E. M., & Umar, R. (2021). Estimating and Monitoring the Land Surface Temperature (LST) Using Landsat OLI 8 TIRS. *International Journal of Environment, Engineering and Education*, *3*(1), 17–24. https://doi.org/10.55151/ijeedu.v3i1.43

Alagaiah Venu, U., & Velmayil, P. (2021a). Texture, mineralogy and geochemistry of Teri sediments from the Kuthiraimozhi deposit, Southern Tamilnadu, India: Implications on provenance, weathering and palaeoclimate. *Arabian Journal of Geosciences*, *14*(5), 364. https://doi.org/10.1007/s12517-021-06549-x

Alagaiah Venu, U., & Velmayil, P. (2021b). Texture, mineralogy and geochemistry of Teri sediments from the Kuthiraimozhi deposit, Southern Tamilnadu, India: Implications on provenance, weathering and palaeoclimate. *Arabian Journal of Geosciences*, *14*(5), 364. https://doi.org/10.1007/s12517-021-06549-x

Alexander, C. (2021). Influence of the proportion, height and proximity of vegetation and buildings on urban land surface temperature. *International Journal of Applied Earth Observation and Geoinformation*, *95*, 102265. https://doi.org/10.1016/j.jag.2020.102265

Asadzadeh, S., & Souza Filho, C. R. (2023). Numerical Modeling of Land Surface Temperature over Complex Geologic Terrains: A Remote Sensing Approach. *Remote Sensing*, *15*(19), 4877. https://doi.org/10.3390/rs15194877

Bobáľová, H., & Opravil, Š. (2026). Improving Landsat land surface temperature estimation in Google Earth Engine using NDVI-based emissivity. *Advances in Space Research*, *77*(3), 3281–3299. https://doi.org/10.1016/j.asr.2025.11.085

Cammalleri, C., & Vogt, J. (2015). On the Role of Land Surface Temperature as Proxy of Soil Moisture Status for Drought Monitoring in Europe. *Remote Sensing*, *7*(12), 16849–16864. https://doi.org/10.3390/rs71215857

Carretero, S., Braga, F., Kruse, E., & Tosi, L. (2014). Temporal analysis of the changes in the sand-dune barrier in the Buenos Aires Province, Argentina, and their relationship with the water resources. *Applied Geography*, *54*, 169–181. https://doi.org/10.1016/j.apgeog.2014.08.004

Ermida, S. L., Soares, P., Mantas, V., Göttsche, F.-M., & Trigo, I. F. (2020). Google Earth Engine Open-Source Code for Land Surface Temperature Estimation from the Landsat Series. *Remote Sensing*, *12*(9), 1471. https://doi.org/10.3390/rs12091471

Faridatul, M. I., Islam, M., Joy, Md. J. H., Wakil, Md. A., Rahman, Md. M., & Sarker, D. (2025). Impact of greenery and waterbody on the cooling of city's environment: A case of Rajshahi City. *Geology, Ecology, and Landscapes*, *9*(3), 1065–1086. https://doi.org/10.1080/24749508.2024.2373489

Feldman, A. F., Short Gianotti, D. J., Dong, J., Trigo, I. F., Salvucci, G. D., & Entekhabi, D. (2023). Tropical surface temperature response to vegetation cover changes and the role of drylands. *Global Change Biology*, *29*(1), 110–125. https://doi.org/10.1111/gcb.16455

Firozjaei, M. K., Kiavarz, M., & Alavipanah, S. K. (2022). Satellite-derived land surface temperature spatial sharpening: A comprehensive review on current status and perspectives. *European Journal of Remote Sensing*, *55*(1), 644–664. https://doi.org/10.1080/22797254.2022.2144764

Głowienka, E., & Kucza, M. (2026). Urban Park Vegetation Indices and Local Cooling in Krakow: A Linear Mixed Effects Model Analysis of Landsat Land Surface Temperature. *IEEE Journal of Selected Topics in Applied Earth Observations and Remote Sensing*, *19*, 6239–6252. https://doi.org/10.1109/JSTARS.2026.3655138

Han, G., Tan, J., Wang, X., Li, H., Shang, Q., & Tian, J. (2025). Response of Soil Temperature to Soil Moisture Content and Meteorological Elements with Gravel-Sand Mulching. *Land*, *14*(4), 853. https://doi.org/10.3390/land14040853

Hasyim, A. W., Sukojo, B. M., Anggraini, I. A., Fatahillah, E. R., & Isdianto, A. (2025). Urban Heat Island Effect and Sustainable Planning: Analysis of Land Surface Temperature and Vegetation in Malang City. *International Journal of Sustainable Development and Planning*, *20*(2), 683–697. https://doi.org/10.18280/ijsdp.200218

Jayangondaperumal, R., Murari, M. K., Sivasubramanian, P., Chandrasekar, N., & Singhvi, A. K. (2012). Luminescence dating of fluvial and coastal red sediments in the SE Coast, India, and implications for paleoenvironmental changes and dune reddening. *Quaternary Research*, *77*(3), 468–481. https://doi.org/10.1016/j.yqres.2012.01.010

Jiang, K., Pan, Z., Pan, F., Teuling, A. J., Han, G., An, P., Chen, X., Wang, J., Song, Y., Cheng, L., Zhang, Z., Huang, N., Ma, S., Gao, R., Zhang, Z., Men, J., Lv, X., & Dong, Z. (2023). Combined influence of soil moisture and atmospheric humidity on land surface temperature under different climatic background. *iScience*, *26*(6), 106837. https://doi.org/10.1016/j.isci.2023.106837

Khan, D., Bano, S., & Khan, N. (2025). Spatio-temporal analysis of urbanization effects: Unravelling land use and land cover dynamics and their influence on land surface temperature in Aligarh City. *Geology, Ecology, and Landscapes*, *9*(4), 1326–1350. https://doi.org/10.1080/24749508.2024.2409488

Li, Z., Wu, H., Duan, S., Zhao, W., Ren, H., Liu, X., Leng, P., Tang, R., Ye, X., Zhu, J., Sun, Y., Si, M., Liu, M., Li, J., Zhang, X., Shang, G., Tang, B., Yan, G., & Zhou, C. (2023). Satellite Remote Sensing of Global Land Surface Temperature: Definition, Methods, Products, and Applications. *Reviews of Geophysics*, *61*(1), e2022RG000777. https://doi.org/10.1029/2022RG000777

Li, Z.-L., Tang, B.-H., Wu, H., Ren, H., Yan, G., Wan, Z., Trigo, I. F., & Sobrino, J. A. (2013). Satellite-derived land surface temperature: Current status and perspectives. *Remote Sensing of Environment*, *131*, 14–37. https://doi.org/10.1016/j.rse.2012.12.008

Mahata, B., Sankar Sahu, S., Sardar, A., Laxmikanta, R., & Maity, M. (2024). Spatiotemporal dynamics of land use/land cover (LULC) changes and its impact on land surface temperature: A case study in New Town Kolkata, eastern India. *Regional Sustainability*, *5*(2), 100138. https://doi.org/10.1016/j.regsus.2024.100138

Mohiuddin, G., & Mund, J.-P. (2023). Spatiotemporal Analysis of Land Surface Temperature in Response to Land Use and Land Cover Changes: A Remote Sensing Approach. *ECRS 2023*, 15. https://doi.org/10.3390/ECRS2023-15836

Morgese, S., Zhang, W., Casale, F., & Bocchiola, D. (2025). A Hydrological–Energy Balance Model to Assess Land Surface Temperature at the Urban Scale: The Case Study of Milano, Italy. *Meteorological Applications*, *32*(3), e70069. https://doi.org/10.1002/met.70069

Nega, W., & Balew, A. (2022). The relationship between land use land cover and land surface temperature using remote sensing: Systematic reviews of studies globally over the past 5 years. *Environmental Science and Pollution Research*, *29*(28), 42493–42508. https://doi.org/10.1007/s11356-022-19997-z

Njoku, E. A., & Tenenbaum, D. E. (2022). Quantitative assessment of the relationship between land use/land cover (LULC), topographic elevation and land surface temperature (LST) in Ilorin, Nigeria. *Remote Sensing Applications: Society and Environment*, *27*, 100780. https://doi.org/10.1016/j.rsase.2022.100780

Patel, S., Indraganti, M., & Jawarneh, R. N. (2024). A comprehensive systematic review: Impact of Land Use/ Land Cover (LULC) on Land Surface Temperatures (LST) and outdoor thermal comfort. *Building and Environment*, *249*, 111130. https://doi.org/10.1016/j.buildenv.2023.111130

Roy, B., & Bari, E. (2022). Examining the relationship between land surface temperature and landscape features using spectral indices with Google Earth Engine. *Heliyon*, *8*(9), e10668. https://doi.org/10.1016/j.heliyon.2022.e10668

Shahfahad, Bindajam, A. A., Naikoo, M. W., Horo, J. P., Mallick, J., Rihan, M., Malcoti, M. D., Talukdar, S., Rahman, R., & Rahman, A. (2023). Response of soil moisture and vegetation conditions in seasonal variation of land surface temperature and surface urban heat island intensity in sub-tropical semi-arid cities. *Theoretical and Applied Climatology*, *153*(1–2), 367–395. https://doi.org/10.1007/s00704-023-04477-2

Singh, S., Kumar, P., Parijat, R., Gonengcil, B., & Rai, A. (2024). Establishing the relationship between land use land cover, normalized difference vegetation index and land surface temperature: A case of Lower Son River Basin, India. *Geography and Sustainability*, *5*(2), 265–275. https://doi.org/10.1016/j.geosus.2023.11.006

Sobrino, J., García-Monteiro, S., & Julien, Y. (2020). Surface Temperature of the Planet Earth from Satellite Data over the Period 2003–2019. *Remote Sensing*, *12*(12), 2036. https://doi.org/10.3390/rs12122036

Taheri, M., Mohammadian, A., Ganji, F., Bigdeli, M., & Nasseri, M. (2022). Energy-Based Approaches in Estimating Actual Evapotranspiration Focusing on Land Surface Temperature: A Review of Methods, Concepts, and Challenges. *Energies*, *15*(4), 1264. https://doi.org/10.3390/en15041264

Tucker, C. J. (1979). Red and photographic infrared linear combinations for monitoring vegetation. *Remote Sensing of Environment*, *8*(2), 127–150. https://doi.org/10.1016/0034-4257(79)90013-0

Ullah, W., Ahmad, K., Ullah, S., Tahir, A. A., Javed, M. F., Nazir, A., Abbasi, A. M., Aziz, M., & Mohamed, A. (2023). Analysis of the relationship among land surface temperature (LST), land use land cover (LULC), and normalized difference vegetation index (NDVI) with topographic elements in the lower Himalayan region. *Heliyon*, *9*(2), e13322. https://doi.org/10.1016/j.heliyon.2023.e13322

V. Muneeswaran & M. Udayakumar. (2022). Woody plant wealth of Therikadu Reserve Forest, Tuticorin, India: A checklist. *Journal of Threatened Taxa*, *14*(9), 21862–21869. https://doi.org/10.11609/jott.7458.14.9.21862-21869

Venugopal, A., Kannan, B., Ganapati, P. S., Krishnan, A., Manikandan, K., Mathiyazhagan, V., & Jayaraman, S. (2024). Nutrient Variability Mapping and Demarcating Management Zones by Employing Fuzzy Clustering in Southern Coastal Region of Tamil Nadu, India. *Sustainability*, *16*(5), 2095. https://doi.org/10.3390/su16052095

Voogt, J. A., & Oke, T. R. (2003). Thermal remote sensing of urban climates. *Remote Sensing of Environment*, *86*(3), 370–384. https://doi.org/10.1016/S0034-4257(03)00079-8

Wang, Y., Xie, X., Zhao, X., Liang, S., Zhu, B., Tursun, A., Jiang, F., Liu, Y., & Zhang, X. (2023). Four-decade response of land surface temperature to urban expansion in Beijing. *Agricultural and Forest Meteorology*, *341*, 109653. https://doi.org/10.1016/j.agrformet.2023.109653

Weng, Q., Lu, D., & Schubring, J. (2004). Estimation of land surface temperature–vegetation abundance relationship for urban heat island studies. *Remote Sensing of Environment*, *89*(4), 467–483. https://doi.org/10.1016/j.rse.2003.11.005

Wu, Q., Li, Z., Yang, C., Li, H., Gong, L., & Guo, F. (2022). On the Scale Effect of Relationship Identification between Land Surface Temperature and 3D Landscape Pattern: The Application of Random Forest. *Remote Sensing*, *14*(2), 279. https://doi.org/10.3390/rs14020279

Xue, Y., Lu, H., Guan, Y., Tian, P., & Yao, T. (2021). Impact of thermal condition on vegetation feedback under greening trend of China. *Science of The Total Environment*, *785*, 147380. https://doi.org/10.1016/j.scitotenv.2021.147380

Yang, Q., Huang, X., Yang, J., & Liu, Y. (2021). The relationship between land surface temperature and artificial impervious surface fraction in 682 global cities: Spatiotemporal variations and drivers. *Environmental Research Letters*, *16*(2), 024032. https://doi.org/10.1088/1748-9326/abdaed

Yang, Y., Anderson, M. C., Gao, F., Wardlow, B., Hain, C. R., Otkin, J. A., Alfieri, J., Yang, Y., Sun, L., & Dulaney, W. (2018). Field-scale mapping of evaporative stress indicators of crop yield: An application over Mead, NE, USA. *Remote Sensing of Environment*, *210*, 387–402. https://doi.org/10.1016/j.rse.2018.02.020

Yao, R., Wang, L., Gui, X., Zheng, Y., Zhang, H., & Huang, X. (2017). Urbanization Effects on Vegetation and Surface Urban Heat Islands in China's Yangtze River Basin. *Remote Sensing*, *9*(6), 540. https://doi.org/10.3390/rs9060540

Zhang, Z., Chen, X., Pan, Z., Zhao, P., Zhang, J., Jiang, K., Wang, J., Han, G., Song, Y., Huang, N., Ma, S., Zhang, J., Yin, W., Zhang, Z., & Men, J. (2022). Quantitative Estimation of the Effects of Soil Moisture on Temperature Using a Soil Water and Heat Coupling Model. *Agriculture*, *12*(9), 1371. https://doi.org/10.3390/agriculture12091371

Zhou, D., Li, D., Sun, G., Zhang, L., Liu, Y., & Hao, L. (2016). Contrasting effects of urbanization and agriculture on surface temperature in eastern China. *Journal of Geophysical Research: Atmospheres*, *121*(16), 9597–9606. https://doi.org/10.1002/2016JD025359

Zhou, S., Zheng, H., Liu, X., Gao, Q., & Xie, J. (2023). Identifying the Effects of Vegetation on Urban Surface Temperatures Based on Urban–Rural Local Climate Zones in a Subtropical Metropolis. *Remote Sensing*, *15*(19), 4743. https://doi.org/10.3390/rs15194743

Ziter, C. D., Pedersen, E. J., Kucharik, C. J., & Turner, M. G. (2019a). Scale-dependent interactions between tree canopy cover and impervious surfaces reduce daytime urban heat during summer. *Proceedings of the National Academy of Sciences*, *116*(15), 7575–7580. https://doi.org/10.1073/pnas.1817561116

Ziter, C. D., Pedersen, E. J., Kucharik, C. J., & Turner, M. G. (2019b). Scale-dependent interactions between tree canopy cover and impervious surfaces reduce daytime urban heat during summer. *Proceedings of the National Academy of Sciences*, *116*(15), 7575–7580. https://doi.org/10.1073/pnas.1817561116